
DECAY PRUNING METHOD: SMOOTH PRUNING WITH A SELF-RECTIFYING PROCEDURE

A PREPRINT

Minghao Yang
Ningbo University
216003669@nbu.edu.cn

Linlin Gao
Ningbo University
gaolinlin@nbu.edu.cn

Pengyuan Li
IBM Research
pengyuandan@ibm.com

Wenbo Li
Zhejiang Lab
liwenbo_923@hotmail.com

Yihong Dong
Ningbo University
dongyihong@nbu.edu.cn

Zhiying Cui
Ningbo University
226004124@nbu.edu.cn

ABSTRACT

Current structured pruning methods often result in considerable accuracy drops due to abrupt network changes and loss of information from pruned structures. To address these issues, we introduce the Decay Pruning Method (DPM), a novel smooth pruning approach with a self-rectifying mechanism. DPM consists of two key components: (i) *Smooth Pruning*: It converts conventional single-step pruning into multi-step smooth pruning, gradually reducing redundant structures to zero over N steps with ongoing optimization. (ii) *Self-Rectifying*: This procedure further enhances the aforementioned process by rectifying sub-optimal pruning decisions based on gradient information. Our approach demonstrates strong generalizability and can be easily integrated with various existing pruning methods. We validate the effectiveness of DPM by integrating it with three popular pruning methods: OTOv2, Depgraph, and Gate Decorator. Experimental results show consistent improvements in performance compared to the original pruning methods, along with further reductions of FLOPs in most scenarios. Our codes are available at https://github.com/Miocio-nora/Decay_Pruning_Method.

1 Introduction

Deep Neural Networks (DNNs) have been widely used for various applications, such as image classification [22; 40], object segmentation [33; 35], and object detection [6; 43]. However, the increasing size and complexity of DNNs often result in substantial computational and memory requirements, posing challenges for deployment on resource-constrained platforms, such as mobile or embedded devices. Consequently, developing efficient methods to reduce the computational complexity and storage demands of large models, while minimizing performance degradation, has become essential.

Network pruning is one of the most popular methods in model compression. Specifically, current network pruning methods are categorized into unstructured and structured pruning [5]. Unstructured pruning [11; 24] focuses on eliminating individual weights from a network to create fine-grained sparsity. Although these approaches achieve an excellent balance between model size reduction and accuracy retention, they often require specific hardware support for acceleration, which is impractical for general-purpose computing environments. Conversely, structured pruning [23; 18; 29] avoids these hardware dependencies by eliminating redundant network structures, thus introducing a more manageable and hardware-compatible form of sparsity. As a result, structured pruning has become popular and is extensively utilized.

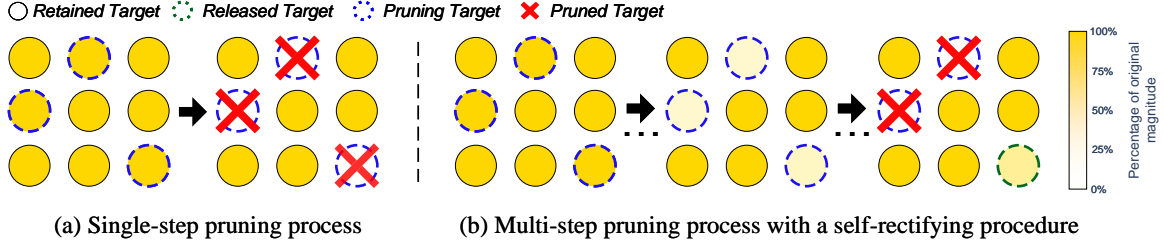


Figure 1: **Single-step pruning vs. Decay pruning method.** (a) Once pruning targets are identified, the single-step pruning process removes them in one action, risking abrupt network changes and irreversible information loss. (b) In contrast, the Decay Pruning Method gradually reduces the weight values of pruning structures over N steps, employing a gradient-driven self-rectifying procedure to identify and rectify sub-optimal decisions.

Existing structured pruning methods fall into two categories based on the granularity of the pruning targets: layer-wise and channel-wise pruning [5]. Layer-wise pruning [1; 32] removes entire layers from a network, which significantly impacts the model performance due to its large-grained nature [45]. On the other hand, channel-wise pruning [2; 10] offers a more fine-grained strategy by removing channels. This method brings less drastic network changes, achieving excellent trade-off between accuracy and model efficiency. Consequently, this paper focuses on channel-wise pruning.

However, current channel-wise pruning methods often apply a single-step pruning process, where redundant structures, once identified, are immediately removed or set to zero in a single operation. Figure 1a shows an illustration of typical single-step pruning process. This approach often encounters several critical challenges:

- (1) **Accuracy damage from abrupt pruning:** Single-step pruning removes redundant network structures drastically, leading to unavoidable information loss and abrupt network changes. These abrupt losses and changes often result in a reduction in model performance, which is particularly hard to recover when pruning large-scale structures, even with subsequent fine-tuning [45].
- (2) **Sub-optimal identification of redundant structures:** Furthermore, the single-step process typically bases its pruning decisions on the current state or gradient information from a single batch [10; 4]. Such an approach overlooks networks’ future evolution and is susceptible to noise or peculiarities in the current data, leading to sub-optimal pruning decisions.

Soft Filter Pruning (SFP) [15] and various dynamic pruning strategies [26; 9] have been developed to mitigate these issues by allowing for the optimization of pruned structures for better information retaining, or enabling the regrowth of mistakenly pruned structures for improved decision-making. However, their persistent reliance on the single-step pruning process limits their effectiveness in fully addressing these challenges.

In response, we propose Decay Pruning Method (DPM), a novel multi-step smooth pruning approach with a self-rectifying procedure. A high-level illustration of our DPM is shown in Figure 1b. Specifically, DPM includes two main components: (i) **Smooth Pruning (SP)**: This procedure gradually decays the weights of redundant structures to zero over N steps while maintaining continuous optimization. This gradual approach avoids abrupt changes to the network and improves information retention during pruning. (ii) **Self-Rectifying (SR)**: This procedure utilizes gradient information of the decaying structures to dynamically identify and rectify sub-optimal pruning decisions. This approach takes into account the network’s future evolving state, ensuring more reliable and adaptive pruning decisions. Our DPM can be seamlessly integrated into various existing pruning frameworks, resulting in significant accuracy improvements and further reductions in FLOPs compared to original pruning methods. We evaluate the effectiveness and generalizability of DPM across multiple pruning frameworks, including two auto pruning frameworks, OTOv2 [4] and Depgraph [10], as well as the classic method Gate Decorator [42]. Our main contributions are as follows:

- We introduce the *SP* procedure, a multi-step pruning process that gradually decays redundant structures to zero over N steps with ongoing optimization. This approach minimizes drastic network changes and enhances information retention during pruning.
- We develop the *SR* procedure, which employs a gradient-driven approach to effectively correct sub-optimal pruning decisions, enabling more adaptive and optimal pruning decisions.
- We demonstrate the effectiveness and generalizability of the proposed DPM by integrating it with three distinct pruning frameworks. Each integration showcases consistent improvements in accuracy and reductions in FLOPs, underscoring DPM’s versatility and significant enhancements across various existing pruning methods.

2 Related Work

Soft pruning methods. Several methods are designed to mitigate information loss from pruned structures by enabling more gentle pruning processes. For instance, SFP [15] allows the ongoing optimization of pruned weights in subsequent epochs to aid in network recovery. Building upon SFP, ASFP [14] enhances information retention by gradually raising pruning rate throughout each iteration of pruning. However, the application of a single-step pruning process in these methods — immediately zeroing out pruned filters — results in irreversible information loss and abrupt network changes. Our DPM addresses these drawbacks by progressively reducing the weights of pruning filters to zero, alongside continuous optimization, ensuring improved information preservation and better network adaptation.

Dynamic pruning methods. Dynamic pruning approaches, such as [26; 9], dynamically prune and regrow network weights to explore optimal sparsity configurations. These methods are effective at correcting sub-optimal pruning decisions by enabling the regeneration of erroneously pruned weights. However, these methods mainly focus on unstructured pruning and typically employ a single-step pruning process. Building upon these concepts, our proposed *Self-Rectifying (SR)* procedure leverages gradient information to dynamically identify and correct sub-optimal pruning decisions within a multi-step pruning process. Our approach not only offers a robust, gradient-based criterion for dynamic adjustments but also seamlessly integrates with various existing structured pruning methods to enhance their effectiveness.

Auto pruning methods. Auto pruning frameworks has been popular these year, due to their advantages of easy deployment and generalizability towards various networks. OTOv2 [4] is a user-friendly auto pruning framework that prunes while training and without fine-tuning. Given a network, OTOv2 automatically divides it into several zero invariant groups, and prunes these groups with their gradient information while training using a DHSPG strategy. Different from OTOv2, Depgraph [10] prunes network through classic iteration of pruning and fine-tuning. This method prunes groups with its own global wise criteria with sparse learning, while also supporting extra criteria including L1, L2, bn scalar and more. APIB [12] is a novel auto pruning method that prunes with a complex criteria based on Information Bottleneck Principle and achieved state-of-the-art results.

3 Decay Pruning Method

This section introduces the Decay Pruning Method (DPM), which consists of two key components: *Smooth Pruning (SP)* and *Self-Rectifying (SR)*. Specifically, *SP* replaces traditional single-step pruning, and applies a multi-step pruning process, gradually decaying weights of redundant structures to zero over N steps with ongoing optimization. Meanwhile, *SR* utilizes gradient information from the decaying weights to adaptively identify and correct sub-optimal pruning decisions, considering the ongoing evolution of the network.

3.1 Smooth Pruning Procedure

SP innovates beyond traditional single-step pruning methods by employing a more gradual N -step process. Given a pruning structure characterized by its weight matrix \mathbf{x} , *SP* begins by measuring its current L2 norm as the initial length, denoted as $L_{init} := \|\mathbf{x}\|_2$. Rather than abruptly removing the weights \mathbf{x} , *SP* gradually reduces them to zeros across N iterations, each coinciding with an subsequent optimization step in the fine-tuning phase. Specifically, at the k^{th} optimization step, where \mathbf{x}_k represents the current state of the weights, *SP* first updates \mathbf{x}_k to a temporary state as $\tilde{\mathbf{x}}_{k+1} := \mathbf{x}_k - a_k \mathbf{g}(\mathbf{x}_k)$ using a general optimizer, where a_k is the learning rate and $\mathbf{g}(\mathbf{x}_k)$ represents the gradient of \mathbf{x}_k . It then obtains \mathbf{x}_{k+1} by scaling $\tilde{\mathbf{x}}_{k+1}$ to a specified L2 norm, L_{target} . This scaling preserves the directional integrity of the weights, ensuring a continuing directional optimization:

$$\mathbf{x}_{k+1} \leftarrow \tilde{\mathbf{x}}_{k+1} \times \frac{L_{target}}{\|\tilde{\mathbf{x}}_{k+1}\|_2} \quad (1)$$

To ensure a consistent decrement in weight magnitude across iterations, L_{target} is derived for each iteration based on the progression through the N -step process, adhering to the following formula:

$$L_{target} := (N - n_{step}) \times L_s, \quad (2)$$

where n_{step} indicates the current iteration step within the decaying process, systematically increasing from 1 to N . This formula emphasizes the sequential reduction in weight magnitude, with L_s dictating the decrement length per iteration. L_s itself is calculated from the initial L2 norm L_{init} , divided by the total decaying steps N :

$$L_s := \frac{L_{init}}{N} \quad (3)$$

Overall, *SP* ensures an equal reduction in the magnitude of \mathbf{x} across N iterations. Upon reaching the final step ($n_step = N$), \mathbf{x} is zeroed out as $L_{target} = 0$, marking its last update. Otherwise, *SP* concludes the current iteration by incrementing n_step by one for next iteration of decaying. Therefore, *SP* achieves a gradual reduction in magnitude of pruning structures while facilitating an ongoing directional optimization, which ultimately enhances the network adaptability towards pruning and better information retention.

Figure 2 illustrates an example of the *SP* procedure with $N = 3$. This figure shows how the weights \mathbf{x}_k are gradually reduced to zero over three optimization steps. The semi-circular dashed lines indicate the potential ranges where \mathbf{x}_k can land at each decaying step, constrained by L_{target} . Initially, at Step-0, *SP* begins the decaying process by recording the current L2 norm as $L_{init} := \|\mathbf{x}_k\|_2$. In the subsequent optimization steps, *SP* first pre-updates \mathbf{x}_k to $\tilde{\mathbf{x}}_{k+1} \leftarrow \mathbf{x}_k - a_k \mathbf{g}(\mathbf{x}_k)$. Following this, *SP* scales $\tilde{\mathbf{x}}_{k+1}$ to \mathbf{x}_{k+1} according to Equation 1, aiming for the decayed L2 norm L_{target} , as specified by the Equation 2. This iterative reduction of \mathbf{x}_k continues until it reaches zero by Step-3, marking its last update.

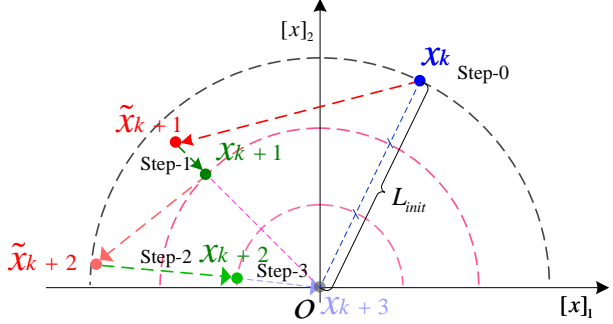


Figure 2: An illustration of the smooth pruning procedure (*SP*) with $N = 3$.

During the decaying process, a specific condition occurs

when the optimized weights $\tilde{\mathbf{x}}_{k+1}$ already meet or fall below the intended L_{target} , evidenced by $\|\tilde{\mathbf{x}}_{k+1}\|_2 \leq L_{target}$. In such instances, further scaling $\tilde{\mathbf{x}}_{k+1}$ to match L_{target} becomes unnecessary. Therefore, *SP* directly updates \mathbf{x}_{k+1} as $\tilde{\mathbf{x}}_{k+1}$ without any additional modification. This iteration concludes by recalibrating the current step (n_step) to align with $\|\tilde{\mathbf{x}}_{k+1}\|_2 \leq L_{target} \leftarrow (N - n_step) \times L_s$ for the next iteration, thereby maintaining efficient weight reduction.

3.2 Self-Rectifying Procedure

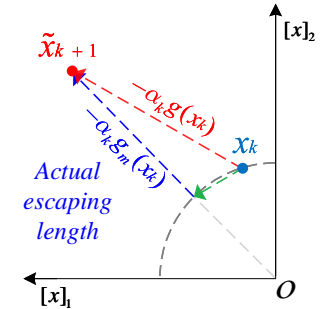
SR leverages gradient information to identify and rectify sub-optimal pruning decisions within the *SP* procedure. Specifically, at the k^{th} optimization step, the gradient $\mathbf{g}(\mathbf{x}_k)$ of the weights \mathbf{x}_k is decomposed into two components: the direction-wise component $\mathbf{g}_d(\mathbf{x}_k)$ and the magnitude-wise component $\mathbf{g}_m(\mathbf{x}_k)$. These components optimize the direction and magnitude of the weights \mathbf{x}_k , respectively. Within the *SP* procedure, while optimization is allowed directionally, the magnitude of the pruning structures is compulsorily reduced. During this process, if an important structure is incorrectly pruned, or the pruning decisions become less optimal due to network evolution, a strong $\mathbf{g}_m(\mathbf{x}_k)$ may emerge, attempting to restore the magnitude of the weights. This strong $\mathbf{g}_m(\mathbf{x}_k)$ indicates resistance against the ongoing decay. Two criteria are proposed to measure $\mathbf{g}_m(\mathbf{x}_k)$ for timely identification and adjustment of sub-optimal pruning decisions.

Criterion 1: Actual Escaping Rate. To assess the resistance to pruning, we define the Actual Escaping Length as $\|\tilde{\mathbf{x}}_{k+1}\|_2 - \|\mathbf{x}_k\|_2$. This measure, representing the increase in the L2 norm of the updated weights $\tilde{\mathbf{x}}_{k+1}$ driven by $\mathbf{g}_m(\mathbf{x}_k)$, also indicates the resistance against the decaying process, as illustrated in Figure 3. Given the variability in gradient magnitude across different layers and training phases, directly employing this measurement as a criterion could result in inconsistencies. To mitigate this, we introduce the Actual Escaping Rate (C_{rate}), which normalizes the Actual Escaping Length by the total impact of the gradient on the weights:

$$C_{rate} := \frac{\|\tilde{\mathbf{x}}_{k+1}\|_2 - \|\mathbf{x}_k\|_2}{\|\tilde{\mathbf{x}}_{k+1} - \mathbf{x}_k\|_2}$$

In this equation, the denominator represents the L2 norm of the total gradient impact, $a_k \mathbf{g}(\mathbf{x}_k)$, depicted as the red line in Figure 3. The numerator captures the change in L2 norm of the weights induced by $a_k \mathbf{g}_m(\mathbf{x}_k)$, depicted as the blue line in Figure 3. This equation ensures that C_{rate} provides a stable measurement of resistance to decay across various layers and training phases. A higher C_{rate} suggests a stronger resistance to the pruning process, potentially indicating a need to release the weights from further decay.

Criterion 2: Magnitude of Gradient. While a high C_{rate} can indicate significant resistance to pruning, the magnitude of the gradients should also be considered. However, C_{rate} can not directly identify short gradients. For instance, a small gradient holding the same direction with the vector pointing from zero to \mathbf{x}_k , can still yield a high C_{rate} of 1, indicating only weak escaping strength and potentially leading to erroneous releases. As such, we designed a dynamic criterion, denoted as C_{len} , which measures the relative magnitude of the gradient compared to its counterparts in



(4) Figure 3: Illustrations of Actual escaping length.

parallel channels within the same layer. Specifically, we calculate the mean magnitude of the gradient across parallel channels that share similar structures and weight magnitudes. The C_{len} is defined as follow:

$$C_{len} := \frac{\|\mathbf{g}(\mathbf{x}_k)\|_2}{\frac{1}{M} \sum_{j=1}^M \|\mathbf{g}(\mathbf{x}_k^j)\|_2}, \quad (5)$$

where M represents the number of parallel channels in the same layer, and \mathbf{x}^j denotes their respective weights. This criterion assesses the strength of the current gradient relative to the parallel gradients, complementing Criterion 1 by setting a dynamic threshold to ensure substantial escaping strength.

Finally, two hyperparameters, T_{rate} and T_{len} , are used to determine if the decaying weights \mathbf{x}_k should be released from the pruning process based on the following condition:

$$C_{rate} > T_{rate} \quad \wedge \quad C_{len} > T_{len}, \quad (6)$$

where \wedge refers to the logical ‘‘AND’’ operation. Once \mathbf{x}_k is released from decaying, it returned to normal optimization. The releasing rate can be adjusted by modifying T_{rate} and T_{len} .

Special Situations. Some pruning methods apply magnitude penalization while fine-tuning. This approach generates an additional force directly targeting zero counteracts most of the escaping strength from the original gradient. Consequently, this results in a low C_{rate} , complicating the trigger for releasing. In response to this situation, we can either neutralize the effect of penalization when computing $\tilde{\mathbf{x}}_i$ or consider setting a lower T_{rate} .

3.3 DPM Integration

In this section, we discuss the integration of the Decay Pruning Method into existing pruning frameworks to enhance their efficacy by replacing the conventional single-step pruning process. Given a model \mathcal{M} , and its structures $\mathbf{x}^i \in \mathcal{M}$, general pruning methods usually follow a three-stage iteration process: (i) *Discovering Pruning Decisions (P)*: Decide which structures to prune. (ii) *Removing Redundant Structures ($\mathbf{x}^i \in P$)*: Remove the identified redundant structures. (iii) *Fine-Tuning Networks*: Adjust the network to recover performance after pruning. Typically, the single-step pruning process operates stage (i) and (ii) concurrently, directly removing identified redundant structures. Differently, DPM modifies this process by interleaving the removal of redundant structures (stage (ii)) within the fine-tuning phase (stage (iii)). This adjustment allows for a more gradual removal of structures over N steps, facilitating a better identification for redundant structures. Specifically, DPM consists of an *Initial Phase*, followed by an iterative *Pruning Decision Phase* and a *Decay Pruning Phase* that prunes while fine-tuning.

Algorithm 1 Outline of the *Pruning Decision Phase*.

```

1: Pruning Decision Phase:
2: Make pruning decision list  $P$ ;
3: for  $\mathbf{x}^i \in \mathcal{M}$  do
4:   if  $\mathbf{x}^i \in P$  then
5:     Project  $\mathbf{x}^i$  to zero and never update.
6:     Initialize decay process for  $\mathbf{x}^i$  if not already decaying:
7:     if not  $is\_decay^i$  then
8:        $L_{init}^i \leftarrow \|\mathbf{x}^i\|_2$ ;
9:        $is\_decay^i \leftarrow True$ ; ▷ Set decay
10:    end if
11:  end if
12: end for

```

Initial Phase. DPM initializes three variables for each structure \mathbf{x}^i , including: $n_step^i := 0$, tracking the number of the decaying steps for the structure; $L_{init}^i := 0$, denoting the initial L2 norm of the structure; and $is_decay^i := False$, indicating whether the structure is currently undergoing decay.

Pruning Decision Phase (Algorithm 1). During each iteration, DPM calculates the current L2 norm of each redundant structure $\mathbf{x}^i \in P$, storing it as L_{init}^i , and sets their is_decay^i as *True*, marking the beginning of the decaying process.

Decay Pruning Phase (Algorithm 2). DPM progressively reduces the magnitude of the redundant structures during optimization steps, in parallel with fine-tuning. Specifically, at the k^{th} optimization step, for a given decaying structure

\mathbf{x}_k^i , DPM initially pre-updates it to $\tilde{\mathbf{x}}_{k+1}^i$ using standard optimization. After that, two criteria: C_{rate} and C_{len} , are calculated based on gradient information to determine whether to continue the decay. If both criteria are met, the decay is halted, and \mathbf{x}^i is released from the decaying process, returning to the normal optimization process. Otherwise, SP projects $\tilde{\mathbf{x}}_{k+1}^i$ to achieve a predetermined L_{target} , and ultimately updates \mathbf{x}_{k+1}^i with $\tilde{\mathbf{x}}_{k+1}^i$. This iterative process continues until \mathbf{x}^i fully decays to zero, after which \mathbf{x}^i is either no longer updated or is directly removed from the model.

Algorithm 2 Outline of the *Decay Pruning Phase*.

```

1: In the  $k^{th}$  optimization step of fine-tuning:
2: for weights  $\mathbf{x}_k^i \in \mathcal{M}$  do
3:   Pre-update  $\mathbf{x}_k^i$  as  $\tilde{\mathbf{x}}_{k+1}^i := \mathbf{x}_k^i - a_k \mathbf{g}(\mathbf{x}_k^i)$ .
4:   if  $is\_decay^i = True$  then
5:     if  $n\_step^i = N$  then
6:        $\tilde{\mathbf{x}}_{k+1}^i \leftarrow 0$ 
7:     else if  $n\_step^i < N$  then
8:       Compute  $C_{rate}$  and  $C_{len}$  using gradients. ▷ See Eqns. 4, 5
9:       if  $C_{rate} > T_{rate} \wedge C_{len} > T_{len}$  then ▷ Condition 6
10:        Release  $\mathbf{x}_k^i$  from decaying:
11:          $is\_decay^i \leftarrow False$ 
12:          $n\_step^i \leftarrow 0$ 
13:       else
14:          $L_s := \frac{L_{init}^i}{N}$  ▷ Eqn 3
15:          $L_{target} := (N - n\_step^i) \times L_s$  ▷ Eqn 2
16:         Project  $\tilde{\mathbf{x}}_{k+1}^i \leftarrow \tilde{\mathbf{x}}_{k+1}^i \times \frac{L_{target}}{\|\tilde{\mathbf{x}}_{k+1}^i\|_2}$  ▷ Eqn 1
17:          $n\_step^i \leftarrow n\_step^i + 1$ 
18:       end if
19:     end if
20:   end if
21:   Update  $\mathbf{x}_{k+1}^i \leftarrow \tilde{\mathbf{x}}_{k+1}^i$ .
22: end for

```

4 Experiment

In this section, we demonstrate the effectiveness and generalizability capabilities of the Decay Pruning Method (DPM) by integrating it with various pruning frameworks, including the auto-pruning frameworks OTOv2 [4] and Depgraph [10], as well as the conventional pruning method, Gate Decorator [42]. We conducted comprehensive experiments across various models such as VGG16 [34], VGG19, ResNet50 [13], and ResNet56 [13], utilizing well-known datasets including CIFAR10 [21], CIFAR100 [21], and ImageNet [7]. These experiments adhered strictly to the original training settings and codes to ensure a valid comparison of DPM’s enhancements.

For the hyperparameter in SP , we set the decaying step N to 5. For the two criterion hyperparameters in SR , T_{rate} is set between [0.2, 0.65], with different values for different methods and datasets, while T_{len} is fixed to 0.2 across all approaches and datasets. This ensures that only structures with significant resistance are released from the pruning process. For methods utilizing sparse learning like L1 or L2 penalization, these hyperparameters are set to lower values: 0.1 to 0.2 for T_{rate} and 0.1 for T_{len} , reducing the impact on the gradient magnitude component \mathbf{g}_m . For further details on hyperparameter validation, please refer to Appendix A.

Our experiments utilized NVIDIA RTX4090 GPUs. In this section, we use ‘+ SP ’ to denote the exclusive use of SP , and ‘+ SR ’ when both SP and SR are applied to each pruning method. We also benchmarked against various state-of-the-art methods, with results cited from the corresponding literature. Cases with unreported results were noted with ‘-’, and the best pruning results are marked in bold.

4.1 Integrating DPM with OTOv2

OTOv2 [4] is a popular auto-pruning method that prunes network while training, without any additional fine-tuning. This method applies a single-step pruning process, directly projecting the redundant structures to zeros and never

update. We enhanced OTOv2 by replacing its single-step pruning process with *SP*, and introduce *SR* to distinguish and rectify sub-optimal pruning decisions utilizing gradient information. To validate the effectiveness of these innovations, we replicated key experiments from OTOv2, including trials with VGG16 on CIFAR10, VGG16-BN on CIFAR10, ResNet50 on CIFAR10, and ResNet50 on ImageNet. These experiments were conducted using the original training codes and maintained consistent hyperparameter settings.

Table 1: VGG16 and VGG16-BN on CIFAR10.

Method	BN	FLOPs	Params	Top-1 Acc.	Method	BN	FLOPs	Params	Top-1 Acc.
Baseline	✗	100%	100%	91.6%	Baseline	✓	100%	100%	93.2%
SBP [31]	✗	31.1%	5.9%	91.0%	EC [23]	✓	65.8%	37.0%	93.1%
BC [28]	✗	38.5%	5.4%	91.0%	Hinge [25]	✓	60.9%	20.0%	93.6%
RBC [44]	✗	32.3%	3.9%	90.5%	SCP [20]	✓	33.8%	7.0%	93.8%
RBP [44]	✗	28.6%	2.6%	91.0%	OTOv1 [2]	✓	26.8%	5.5%	93.3%
OTOv1 [2]	✗	16.3%	2.5%	91.0%	OTOv3 [3]	✓	26.6%	5.0%	93.4%
OTOv2 [4]	✗	13.0%	2.3%	91.65%	OTOv2 [4]	✓	26.5%	4.8%	93.4%
+ <i>SP</i> (Ours)	✗	13.4%	2.5%	92.11%	+ <i>SP</i> (Ours)	✓	26.4%	4.8%	93.6%
+ <i>SR</i> (Ours)	✗	15.0%	2.8%	92.65%	+ <i>SR</i> (Ours)	✓	25.8%	4.8%	93.8%

VGG16 for CIFAR10. We evaluated DPM on CIFAR10 using both the vanilla VGG16 and a variant known as VGG16-BN, which includes a batch normalization layer after each convolutional layer. The results, presented in Table 1, contrast the original OTOv2 with its enhanced version incorporating DPM. Specifically, for the vanilla VGG16, the *SP* component of DPM yielded a 0.4% boost in accuracy, albeit with a slight increase in FLOPs and parameters. By further incorporating the *SR* component, DPM achieved a noteworthy 1% improvement in accuracy, resulting in a superior accuracy-efficiency trade-off. For the VGG16-BN variant, DPM achieved a top-1 accuracy of 93.8%, utilizing even fewer FLOPs, clearly surpassing the performance of the original OTOv2 and other competitive methods such as OTOv3 and SCP.

ResNet50 for CIFAR10. We evaluated our DPM using ResNet50 on CIFAR10, as detailed in Table 2. While the OTOv2 method already provides state-of-the-art results with extreme pruning rates, DPM has further enhanced this by achieving a better balance between accuracy and model efficiency. Specifically, under 90% group sparsity, DPM impressively reduced the FLOPs to 1.7% and parameters to 0.8%, without sacrificing performance. Under 80% group sparsity, DPM further decreased FLOPs to 6.9% and parameters to 3.1%, while still achieving a top-1 accuracy of 94.7%. These results are highly competitive to other pruning methods such as OTOv1 and N2NSkip, yet achieves 2-3 times more efficiency.

ResNet50 for ImageNet. We assessed the performance of our DPM on the ResNet50 model using the challenging ImageNet dataset. In particular, under 70% group sparsity, DPM achieved a significant 0.84% increase in top-1 accuracy and a 1.32% further reduction in FLOPs compared to the original OTOv2 method. Similarly, under 60% group sparsity, DPM yielded a 0.66% improvement in top-1 accuracy.

Overall, the integration of DPM within the OTOv2 framework underscores its substantial effectiveness in enhancing pruning while training methods. DPM consistently delivers significant improvements by either boosting accuracy or further reducing FLOPs across various benchmarks and pruning rates, setting new state-of-the-art results.

Table 2: ResNet50 on CIFAR10

Method	FLOPs	Params	Top-1 Acc.
Baseline	100%	100%	93.5%
AMC [16]	–	60.0%	93.6%
PruneTrain [30]	30.0%	–	93.1%
N2NSkip [36]	–	10.0%	94.4%
OTOv1 [2]	12.8%	8.8%	94.4%
OTOv2 [4] (90% group sparsity)	2.2%	1.2%	93.0%
+ <i>SP</i> (90% group sparsity)	2.16%	0.84%	92.9%
+ <i>SR</i> (90% group sparsity)	1.7%	0.8%	93.0%
OTOv2 [4] (80% group sparsity)	7.8%	4.1%	94.5%
+ <i>SP</i> (80% group sparsity)	7.8%	3.3%	94.66%
+ <i>SR</i> (80% group sparsity)	6.9%	3.1%	94.70%

Table 3: ResNet50 on ImageNet

Method	FLOPs	Params	Top-1/5 Acc.
Baseline	100%	100%	76.1% / 92.9%
CP [17]	66.7%	–	72.3% / 90.8%
DDS-26 [19]	57.0%	61.2%	71.8% / 91.9%
SFP [15]	41.8%	–	74.6% / 92.1%
RRBP [44]	45.4%	–	73.0% / 91.0%
Group-HS [41]	52.9%	–	76.4% / 93.1%
Hinge [25]	46.6%	–	74.7% / –
SCP [20]	45.7%	–	74.2% / 92.0%
ResRep [8]	45.5%	–	76.2% / 92.9%
OTOv1 [2]	34.5%	35.5%	74.7% / 92.1%
OTOv2 [4] (70% group sparsity)	14.5%	21.3%	70.1% / 89.3%
+ <i>SP</i> (70% group sparsity)	13.8%	22.0%	70.7% / 89.6%
+ <i>SR</i> (70% group sparsity)	13.28%	22.36%	70.94% / 89.63%
OTOv2 [4] (60% group sparsity)	20.0%	28.5%	72.2% / 90.7%
+ <i>SP</i> (60% group sparsity)	20.2%	29.7%	72.75% / 90.9%
+ <i>SR</i> (60% group sparsity)	19.82%	30.1%	72.86% / 90.8%

4.2 Integrating DPM with Depgraph

Depgraph [10] is an automated pruning framework that implements a classic iterative pruning strategy, alternating between pruning and fine-tuning. Given a pruning structure, Depgraph directly removes it from the network, which can result in abrupt network changes and considerable information loss. We address these drawbacks by introducing DPM, which provides a gradually removal of structures and a self-rectifying procedure to adjust pruning decisions adaptively. We integrated DPM with Depgraph following the methodologies outlined in Section 3.3, where structures are only removed once they have fully decayed to zero. Depgraph supports various established pruning criteria, including their own proposed magnitude-based global pruning criteria (Group pruner), both with and without sparse learning, and a group-level batch normalization scalar (BN pruner) adapted from [27]. We have validated the effectiveness of DPM across these criteria using benchmarks such as ResNet56 on CIFAR10 and VGG19 on CIFAR100. For clarity in our results, we denote the use of the Group pruner without sparse learning as ‘w/o SL’.

ResNet56 for CIFAR10. We evaluated DPM-enhanced Depgraph using ResNet56 on the CIFAR10 dataset, employing various criteria. As detailed in Table 4, when utilizing Group pruner with and without sparse learning, DPM significantly boosted accuracy in both scenarios while further reducing parameters by nearly 4%. Notably, for the Group pruner with sparse learning, DPM achieved a new state-of-the-art accuracy of 94.13% while further reducing FLOPs by 1% and parameters by 5.7%. This result clearly surpassed the state-of-the-art method APIB by 0.2% in accuracy, while achieving higher model efficiency. Applying DPM with the BN pruner, a conventional pruning criterion, we observed an additional accuracy improvement of 0.27%. These results underscore the robustness and adaptability of DPM across different pruning criteria and conditions. Moreover, compared to soft pruning methods such as SFP and its enhanced version ASFP, DPM shows a significant surpass in accuracy and FLOP reduction.

VGG19 for CIFAR100. We also validated DPM-enhanced Depgraph with VGG19 on the CIFAR100 dataset, a more challenging benchmark. As shown in Table 6, DPM ultimately provided an accuracy enhancement by 0.18% to the Group pruner, both with and without sparse learning, surpassing other methods in both accuracy and FLOP reduction.

The application of DPM to Depgraph has confirmed the generalizability of *SP* and *SR* across various criteria and conditions, each demonstrating significant improvements from individual perspectives.

4.3 Integrating DPM with Gate Decorator

Gate Decorator [42] is a classic mask-based pruning method that leverages the magnitude of batch normalization (BN) scalars to guide pruning decisions. Unlike the previously discussed auto-pruning frameworks, Gate Decorator groups structures by their BN layers and prunes by zeroing out their BN masks. In our integration with DPM, we decay and assess the gradients from the entire weights of each structure, not just the BN masks. This broader modification provides more robust gradient information for *SR* to accurately identify and release sub-optimal pruning decisions.

We evaluated the DPM-enhanced Gate Decorator on VGG16 and ResNet56 using the CIFAR10 dataset. This integration of DPM resulted in an accuracy increase of 0.19% for ResNet56 and 0.24% for VGG16. Specifically, *SP* contributed

Table 4: ResNet56 on CIFAR10

Method	FLOPs	Params	Top-1 Acc.
Polar [37]	53.2%	–	93.83%
SCP [20]	51.5%	48.47%	93.23%
Hinge [25]	50.0%	48.73%	93.69%
ResRep [8]	47.2%	–	93.71%
APIB [12]	46.0%	50.0%	93.92%
SFP [15]	47.4%	–	93.66%
ASFP [14]	47.4%	–	93.32%
Group pruner	46.86%	52.9%	93.84%
+ <i>SP</i> (Ours)	46.32%	49.69%	93.96%
+ <i>SR</i> (Ours)	45.80%	47.22%	94.13%
Group pruner w/o SL	47.2%	69.7%	93.32%
+ <i>SP</i> (Ours)	46.7%	68.1%	93.62%
+ <i>SR</i> (Ours)	47.1%	65.73%	93.71%
BN pruner	46.4%	58.3%	93.50%
+ <i>SP</i> (Ours)	46.8%	57.3%	93.71%
+ <i>SR</i> (Ours)	46.9%	56.5%	93.77%

Table 5: VGG19 on CIFAR100

Method	FLOPs	Params	Top-1 Acc.
EigenD [38]	11.37%	–	65.18%
GReg-1 [39]	11.31%	–	67.55%
GReg-2 [39]	11.31%	–	67.75%
Group pruner	11.03%	6.36%	70.74%
+ <i>SP</i> (Ours)	10.95%	5.82%	70.85%
+ <i>SR</i> (Ours)	10.86%	6.10%	70.92%
Group pruner w/o SL	11.36%	8.10%	67.58%
+ <i>SP</i> (Ours)	12.06%	7.82%	67.66%
+ <i>SR</i> (Ours)	12.06%	8.36%	67.76%

Table 6: ResNet50 on CIFAR10

Architecture	Method	FLOPs	Params	Top-1 Acc.
ResNet56	Original	29.81%	31.72%	92.63%
	+ <i>SP</i> (Ours)	29.96%	32.11%	92.70%
	+ <i>SR</i> (Ours)	29.80%	32.55%	92.82%
VGG16	Original	9.86%	1.98%	91.50%
	+ <i>SP</i> (Ours)	9.88%	1.97%	91.58%
	+ <i>SR</i> (Ours)	9.79%	1.95%	91.74%

to a more gradual pruning process, which improved accuracy by approximately 0.07%. *SR* further enhanced this by correcting sub-optimal decisions. Notably, for VGG16, *SR* achieved an additional accuracy improvement of 0.16% with higher model efficiency over *SP* by releasing only three sub-optimal pruning decisions. These results underscore the broad applicability and effectiveness of DPM in enhancing mask-based pruning methods.

5 Conclusion

This paper introduced the Decay Pruning Method (DPM), a novel smooth pruning approach that prunes by gradually decaying redundant structures over multiple steps while rectifying sub-optimal pruning decisions using gradient information. Tested across diverse pruning frameworks like OTOv2, Depgraph, and Gate Decorator, DPM has demonstrated exceptional adaptability and effectiveness, improving performance across various pruning strategies and conditions. These results highlight DPM’s potential as a versatile tool that can be embedded on various existing pruning methods and provides significant enhancements.

References

- [1] Shi Chen and Qi Zhao. Shallowing deep networks: Layer-wise pruning based on feature representations, 2019.
- [2] Tianyi Chen, Bo Ji, Tianyu Ding, Biyi Fang, Guanyi Wang, Zhihui Zhu, Luming Liang, Yixin Shi, Sheng Yi, and Xiao Tu. Only train once: A one-shot neural network training and pruning framework. In *Proc. Adv. Neural Inf. Process. Syst.*, pages 19637–19651, 2021.
- [3] Tianyi Chen, Luming Liang, Tianyu Ding, and Ilya Zharkov. Towards automatic neural architecture search within general super-networks. *arXiv preprint arXiv:2305.18030*, 2023.
- [4] Tianyi Chen, Luming Liang, Tianyu Ding, Zhihui Zhu, and Ilya Zharkov. Otov2: Automatic, generic, user-friendly. In *Proc. Int. Conf. Learn. Represent.*, 2023.
- [5] Hongrong Cheng, Miao Zhang, and Javen Qinfeng Shi. A survey on deep neural network pruning-taxonomy, comparison, analysis, and recommendations. *arXiv preprint arXiv/2308.06767*, 2023.
- [6] Tianheng Cheng, Lin Song, Yixiao Ge, Wenyu Liu, Xinggang Wang, and Ying Shan. Yolo-world: Real-time open-vocabulary object detection. In *Proc. IEEE Conf. Comput. Vis. Pattern Recog.*, 2024.
- [7] Jia Deng, Wei Dong, Richard Socher, Li-Jia Li, Kai Li, and Feifei Li. Imagenet: A large-scale hierarchical image database. In *Proc. IEEE Conf. Comput. Vis. Pattern Recog.*, pages 248–255, 2009.
- [8] Xiaohan Ding, Tianxiang Hao, Jianchao Tan, Ji Liu, Jungong Han, Yuchen Guo, and Guiguang Ding. Resrep: Lossless cnn pruning via decoupling remembering and forgetting. In *Proc. IEEE Int. Conf. Comput. Vis.*, pages 4490–4500, 2020.
- [9] Utku Evci, Trevor Gale, Jacob Menick, Pablo Samuel Castro, and Erich Elsen. Rigging the lottery: Making all tickets winners. In *Proc. Int. Conf. Machin. Learn.*, 2020.
- [10] Gongfan Fang, Xinyin Ma, Mingli Song, Michael Bi Mi, and Xinchao Wang. Depgraph: Towards any structural pruning. In *Proc. IEEE Conf. Comput. Vis. Pattern Recog.*, pages 16091–16101, 2023.
- [11] Elias Frantar and Dan Alistarh. SPDY: Accurate pruning with speedup guarantees. In *Proc. Int. Conf. Learn. Represent.*, 2022.
- [12] Song Guo, Lei Zhang, Xiawu Zheng, Yan Wang, Yuchao Li, Fei Chao, Chenglin Wu, Shengchuan Zhang, and Rongrong Ji. Automatic network pruning via hilbert-schmidt independence criterion lasso under information bottleneck principle. In *Proc. IEEE Int. Conf. Comput. Vis.*, pages 17412–17423, 2023.
- [13] Kaiming He, Xiangyu Zhang, Shaoqing Ren, and Jian Sun. Deep residual learning for image recognition. In *Proc. IEEE Conf. Comput. Vis. Pattern Recog.*, 2015.
- [14] Yang He, Xuanyi Dong, Guoliang Kang, Yanwei Fu, Chenggang Yan, and Yi Yang. Asymptotic soft filter pruning for deep convolutional neural networks. *arXiv preprint arXiv:1808.07471*, 2019.
- [15] Yang He, Guoliang Kang, Xuanyi Dong, Yanwei Fu, and Yi Yang. Soft filter pruning for accelerating deep convolutional neural networks. In *Proc. Int. Joint Conf. Artif. Intell.*, 2018.
- [16] Yihui He, Ji Lin, Zhijian Liu, Hanrui Wang, Li-Jia Li, and Song Han. Amc: Automl for model compression and acceleration on mobile devices. In *Proc. Eur. Conf. Comput. Vis.*, 2018.
- [17] Yihui He, Xiangyu Zhang, and Jian Sun. Channel pruning for accelerating very deep neural networks. In *Proc. IEEE Int. Conf. Comput. Vis.*, pages 1398–1406, 2017.

- [18] Hengyuan Hu, Rui Peng, Yu-Wing Tai, and Chi-Keung Tang. Network trimming: A data-driven neuron pruning approach towards efficient deep architectures. *arXiv preprint arXiv:1607.03250*, 2016.
- [19] Zehao Huang, editor="Ferrari Vittorio Wang, Naiyan", Martial Hebert, Cristian Sminchisescu, and Yair Weiss. Data-driven sparse structure selection for deep neural networks. In *Proc. Eur. Conf. Comput. Vis.*, volume 8, pages 317–334, 2018.
- [20] Minsoo Kang and Bohyung Han. Operation-aware soft channel pruning using differentiable masks. In *Proc. Int. Conf. Mach. Learn.*, pages 5122–5131, 2020.
- [21] Alex Krizhevsky. Learning multiple layers of features from tiny images. 2009.
- [22] Chuyi Li, Lulu Li, Yifei Geng, Hongliang Jiang, Meng Cheng, Bo Zhang, Zaidan Ke, Xiaoming Xu, and Xiangxiang Chu. Yolov6 v3.0: A full-scale reloading. *arXiv preprint arXiv:2301.05586*, 2023.
- [23] Hao Li, Asim Kadav, Igor Durdanovic, Hanan Samet, and Hans Peter Graf. Pruning filters for efficient convnets. In *Proc. Int. Conf. Learn. Represent.*, 2017.
- [24] Jiajun Li and Ahmed Louri. Adaprun: An accelerator-aware pruning technique for sustainable cnn accelerators. *IEEE Trans. Sustain. Comput.*, 7(1):47–60, 2022.
- [25] Yawei Li, Shuhang Gu, Christoph Mayer, Luc Van Gool, and Radu Timofte. Group sparsity: The hinge between filter pruning and decomposition for network compression. In *Proc. IEEE Conf. Comput. Vis. Pattern Recog.*, pages 8015–8024, 2020.
- [26] Tao Lin, Sebastian U. Stich, Luis Barba, Daniil Dmitriev, and Martin Jaggi. Dynamic model pruning with feedback. In *Proc. Int. Conf. Learn. Represent.*, 2020.
- [27] Zhuang Liu, Jianguo Li, Zhiqiang Shen, Gao Huang, Shoumeng Yan, and Changshui Zhang. Learning efficient convolutional networks through network slimming. In *Proc. IEEE Int. Conf. Comput. Vis.*, pages 2755–2763, 2017.
- [28] Christos Louizos, Karen Ullrich, and Max Welling. Bayesian compression for deep learning. In *Proc. Adv. Neural Inf. Process. Syst.*, 2017.
- [29] Jian-Hao Luo and Jianxin Wu. An entropy-based pruning method for cnn compression. *arXiv preprint arXiv:1706.05791*, 2017.
- [30] Sangkug Lym, Esha Choukse, Siavash Zangeneh, Wei Wen, Sujay Sanghavi, and Mattan Erez. Prunetrain: fast neural network training by dynamic sparse model reconfiguration. In *Proc. Int. Conf. High Perform. Comput. Netw. Storage Anal.*, 2019.
- [31] Kirill Neklyudov, Dmitry Molchanov, Arsenii Ashukha, and Dmitry P. Vetrov. Structured bayesian pruning via log-normal multiplicative noise. In *Proc. Adv. Neural Inf. Process. Syst.*, 2017.
- [32] Youngmin Ro and Jin Young Choi. Autolr: Layer-wise pruning and auto-tuning of learning rates in fine-tuning of deep networks.
- [33] Olaf Ronneberger, Philipp Fischer, and Thomas Brox. U-net: Convolutional networks for biomedical image segmentation. In *Proc. Med. Image Comput. Comput. Assist. Interv.*, pages 234–241, 2015.
- [34] Karen Simonyan and Andrew Zisserman. Very deep convolutional networks for large-scale image recognition. In *Proc. Int. Conf. Learn. Represent.*, 2015.
- [35] Konstantin Sofiiuk, Ilya A. Petrov, and Anton Konushin. Reviving iterative training with mask guidance for interactive segmentation. In *Proc. IEEE Int. Conf. Image Process.*, pages 3141–3145, 2022.
- [36] Arvind Subramaniam and Avinash Sharma. N2nskip: Learning highly sparse networks using neuron-to-neuron skip connections. In *Proc. Br. Mach. Vis. Conf.*, 2022.
- [37] Zhuang Tao, Zhixuan Zhang, Yuheng Huang, Xiaoyi Zeng, Kai Shuang, and Xiang Li. Neuron-level structured pruning using polarization regularizer. In *Proc. Adv. Neural Inf. Process. Syst.*, 2020.
- [38] Chaoqi Wang, Roger Baker Grosse, Sanja Fidler, and Guodong Zhang. Eigendamage: Structured pruning in the kronecker-factored eigenbasis. In *Proc. Int. Conf. Mach. Learn.*, pages 6566–6575, 2019.
- [39] Huan Wang, Can Qin, Yulun Zhang, and Yun Raymond Fu. Neural pruning via growing regularization. In *Proc. Int. Conf. Learn. Represent.*, 2020.
- [40] Qianqian Wang, Yen-Yu Chang, Ruojin Cai, Zhengqi Li, Bharath Hariharan, Aleksander Holynski, and Noah Snavely. Tracking everything everywhere all at once. In *Proc. IEEE Int. Conf. Comput. Vis.*, pages 19738–19749, 2023.

- [41] Huanrui Yang, Wei Wen, and Hai Helen Li. Deepphoyer: Learning sparser neural network with differentiable scale-invariant sparsity measures. In *Proc. Int. Conf. Learn. Represent.*, 2019.
- [42] Zhonghui You, Kun Yan, Jinmian Ye, Meng Ma, and Ping Wang. Gate decorator: Global filter pruning method for accelerating deep convolutional neural networks. In *Proc. Adv. Neural Inf. Process. Syst.*, pages 2130–2141, 2019.
- [43] Xiangyu Zhao, Yicheng Chen, Shilin Xu, Xiangtai Li, Xinjiang Wang, Yining Li, and Haian Huang. An open and comprehensive pipeline for unified object grounding and detection. *arXiv preprint arXiv:2401.02361*, 2024.
- [44] Yuefu Zhou, Ya Zhang, Yanfeng Wang, and Qi Tian. Accelerate cnn via recursive bayesian pruning. In *Proc. IEEE Int. Conf. Comput. Vis.*, pages 3305–3314, 2018.
- [45] Michael Zhu and Suyog Gupta. To prune, or not to prune: exploring the efficacy of pruning for model compression. *arXiv preprint arXiv:1710.01878*, 2017.

A Hyperparameter Verification

In this appendix, we explore the effects of hyperparameters of DPM, including the decaying step N for SP , and two thresholds T_{rate} and T_{len} for SR , verifying them on benchmarks with OTOv2 and Depgraph.

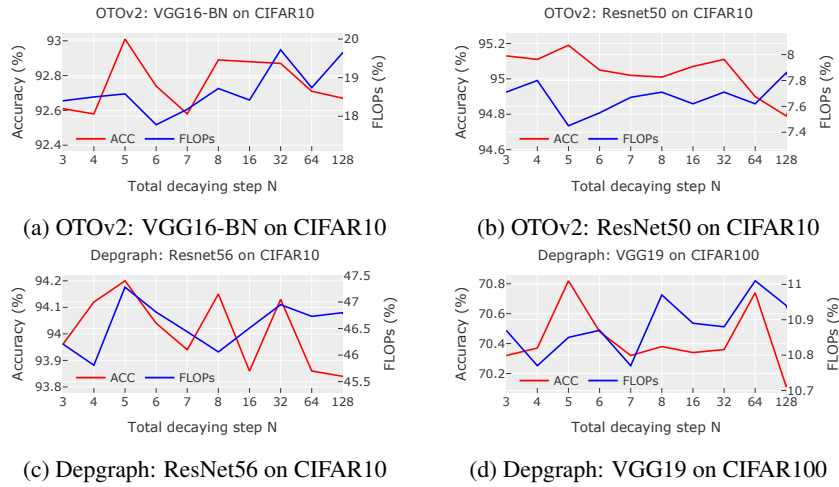


Figure 4: Illustrations of the impact of varying decaying step N from 3 to 128. Red lines indicate the accuracy, and blue lines represent the FLOPs of the pruned networks.

1) **Hyperparameter N :** This hyperparameter dictates the number of the optimization steps that SP utilizes to decay a pruning structure to zero. We vary N from 3 to 128 to encompass both small and large value conditions. The experiments are conducted on four different benchmarks for OTOv2 and Depgraph, focusing on only SP -enhanced conditions. The results are depicted in Fig. 4. We find that setting N too high leads to diminished accuracy and increased computational and time overheads. Thus, smaller N is encouraged. Overall, setting N to 5 brings in the highest accuracy and relatively low FLOPs from Fig. 4(a)-(d), providing a better trade-off between pruning performance and efficiency.

2) **Hyperparameters T_{rate} and T_{len} :** These two hyperparameters govern the release amount for sub-optimal pruning structures in the SR procedure. We varied both hyperparameters from 0.1 to 1, with increments of 0.1. Results are presented only for cases where the released amount exceeded 0, indicating that SR effectively influenced the outcomes. To assess the individual impact of each hyperparameter, we conducted evaluations by setting one parameter to zero while adjusting the other, with the decaying step fixed at $N = 5$. This setting allows us to isolate and observe the effects of T_{rate} and T_{len} on accuracy, FLOPs, and released amounts. The hyperparameters were evaluated with OTOv2 and Depgraph on two well-established benchmarks: VGG16 on CIFAR10 and VGG19 on CIFAR100. The experimental results are shown in Fig. 5.

By comparing Fig. 5a and 5c with Fig. 5b and 5d, we observe that T_{rate} provides a more significant and stable improvement in accuracy compared to T_{len} . This indicates that the proposed Actual Escaping Rate offers a more effective criterion for optimal pruning decisions than methods relying solely on gradient magnitude. Moreover, as shown in 5b and 5d, the proposed dynamic gradient magnitude, T_{len} , results in noticeable accuracy gains especially at a

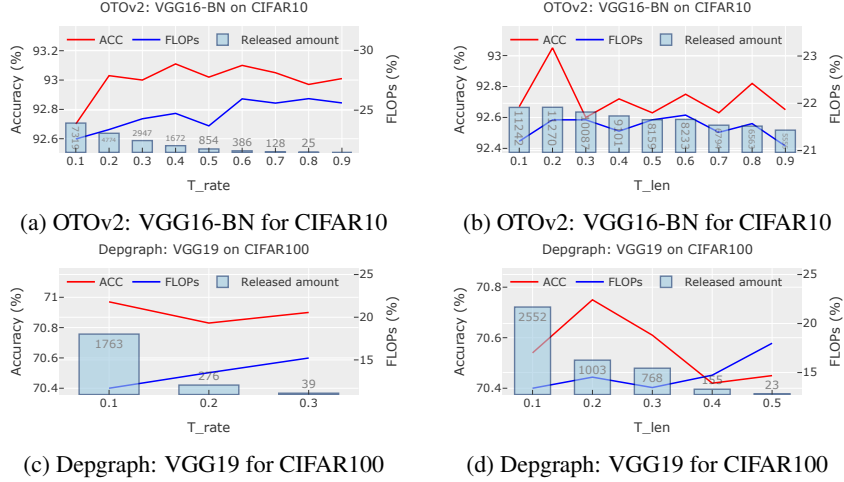


Figure 5: Illustrations of the impact of varying T_{rate} and T_{len} . Red lines indicate the accuracy, and blue lines represent the FLOPs of the pruned networks. The total released amount is depicted with histograms.

small setting of 0.2. This setting ensures that the gradient magnitude remains sufficient to complement T_{rate} , leading to enhanced and stable improvements in accuracy. Based on these findings, we recommend setting T_{len} initially to a smaller value, such as 0.1 or 0.2, and adjusting T_{rate} to effectively control the release amount during the pruning process.

B Pruning Efficiency Analysis of DPM

This section demonstrates the pruning efficiency of the *SP* and *SR* procedure of the Decay Pruning Method (DPM). We assess these components individually by tracking the progression of network sparsity and the amount of structures released by *SR* during the pruning process. Our analysis encompasses tests on four benchmarks using OTOv2 and Depgraph, with each configured to $N = 5$ and low values settings for T_{rate} and T_{len} to trigger numerous releases.

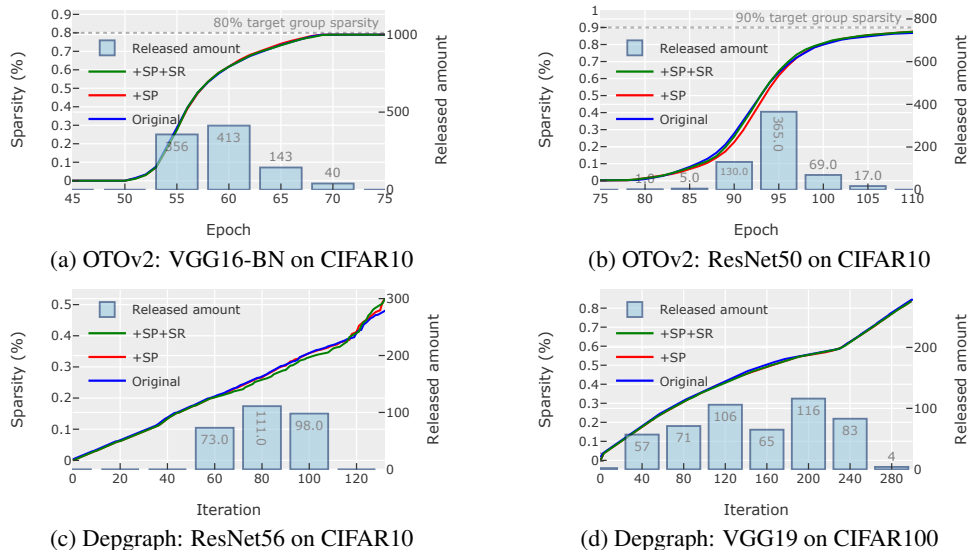


Figure 6: Illustration of group sparsity growth during pruning with *SP* and *SR* compared to the original methods. Blue lines represent the original method, while red and green lines indicate the implementations of *SP* and *SP* with *SR*, respectively. The released amount of *SR* accumulated over a certain period is depicted with histograms.

As illustrated in Figure 6, with five steps of decaying, *SP* achieved target sparsity nearly concurrently with the original method, without imposing significant overheads during fine-tuning. Additionally, *SR* effectively rectified hundreds of

sub-optimal pruning decisions while still maintaining a high pruning efficiency, with slight or even reduced overheads compared to the original method. Notably, since DPM leverages the fine-tuning phase inherent in the original pruning strategies (e.g., the training phase of OTOv2, which also serves as a fine-tuning phase for pruned structures), it does not necessitate an additional fine-tuning phase. This integration ensures that DPM not only enhances accuracy significantly but also preserves the efficiency of the pruning process.